

Key Points:

- This study compared two methods of determining fuel load and fuel consumption for two wildfires in the inland northwest
- LANDFIRE Fuel Characteristics Classification Systems overestimated fuel load and consumption compared to airborne laser scanning
- Much of the difference was attributed to the difference in scale between the two approaches

Supporting Information:

Supporting Information may be found in the online version of this article.

Correspondence to:

T. R. McCarley,
tmccarley@uidaho.edu

Citation:

McCarley, T. R., Hudak, A. T., Restaino, J. C., Billmire, M., French, N. H. F., Ottmar, R. D., et al. (2022). A comparison of multitemporal airborne laser scanning data and the Fuel Characteristics Classification System for estimating fuel load and consumption. *Journal of Geophysical Research: Biogeosciences*, 127, e2021JG006733. <https://doi.org/10.1029/2021JG006733>

Received 23 NOV 2021

Accepted 6 MAY 2022

Author Contributions:

Conceptualization: T. Ryan McCarley, Andrew T. Hudak, Joseph C. Restaino

Data curation: T. Ryan McCarley, Joseph C. Restaino, Michael Billmire, Bridget Hass, Kyle Zarzana, Tristan Goulden, Rainer Volkamer

Formal analysis: T. Ryan McCarley, Joseph C. Restaino

Funding acquisition: Andrew T. Hudak, Roger D. Ottmar, Rainer Volkamer









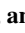

Investigation: T. Ryan McCarley, Andrew T. Hudak, Joseph C. Restaino

Methodology: T. Ryan McCarley, Andrew T. Hudak, Joseph C. Restaino, Nancy H. F. French

Project Administration: Andrew T. Hudak, Roger D. Ottmar

© 2022. American Geophysical Union.
 All Rights Reserved.

A Comparison of Multitemporal Airborne Laser Scanning Data and the Fuel Characteristics Classification System for Estimating Fuel Load and Consumption

T. Ryan McCarley¹ , Andrew T. Hudak² , Joseph C. Restaino³ , Michael Billmire⁴ , Nancy H. F. French⁴ , Roger D. Ottmar⁵ , Bridget Hass⁶ , Kyle Zarzana⁷ , Tristan Goulden⁶ , and Rainer Volkamer⁷ 

¹University of Idaho, College of Natural Resources, Moscow, ID, USA, ²U.S. Department of Agriculture Forest Service, Rocky Mountain Research Station, Moscow, ID, USA, ³California Department of Forestry and Fire Protection, Fire and Resource Assessment Program, South Lake Tahoe, CA, USA, ⁴Michigan Tech Research Institute, Michigan Technological University, Ann Arbor, MI, USA, ⁵U.S. Department of Agriculture Forest Service, Pacific Northwest Research Station, Seattle, WA, USA, ⁶National Ecological Observatory Network, Boulder, CO, USA, ⁷Department of Chemistry & Cooperative Institute for Research in Environmental Sciences (CIRES), University of Colorado Boulder, Boulder, CO, USA

Abstract Characterizing pre-fire fuel load and fuel consumption are critical for assessing fire behavior, fire effects, and smoke emissions. Two approaches for quantifying fuel load are airborne laser scanning (ALS) and the Fuel Characteristic Classification System (FCCS). The implementation of multitemporal ALS (i.e., the use of two or more ALS datasets across time at a given location) in conjunction with empirical models trained with field data can be used to measure fuel and estimate fuel consumption from a fire. FCCS, adapted for use in LANDFIRE (LF), provides 30 m resolution estimates of fuel load across the contiguous United States and can be used to estimate fuel consumption through software programs such as Fuel and Fire Tools (FFT). This study compares the two approaches for two wildfires in the northwestern United States having predominantly sagebrush steppe and ponderosa pine savanna ecosystems. The results showed that the LF FCCS approach yielded higher pre-fire fuel loads and fuel consumption than the ALS approach and that the coarser scale LF FCCS data did not capture as much heterogeneity as the ALS data. At Tepee, 50.0% of the difference in fuel load and 87.3% of the difference in fuel consumption were associated with distinguishing sparse trees from rangeland. At Keithly, this only accounted for 8.2% and 8.6% of the differences, demonstrating the significance of capturing heterogeneity in rangeland vegetation structure and fire effects. Our results suggest future opportunities to use ALS data to better parametrize fine-scale fuel load variability that LF FCCS does not capture.

Plain Language Summary The ability to quantify live and dead vegetation, also known as fuel available to burn in a fire, is important for understanding fire behavior, fire effects, and smoke emissions. Our study compares two methods of measuring pre-fire fuel and estimating the amount of fuel consumed at two wildfires in the northwestern U.S. dominated by sagebrush, grassland, and pine savanna. One method, airborne laser scanning (ALS), uses an aircraft mounted sensor to create detailed 3D maps of vegetation structure. Flights before and after the fire are used to estimate fuel consumption. The other method, the Fuel Characteristic Classification System (FCCS), is a predefined map of fuels and their distinguishing characteristics, which can be easily fed into existing mathematical models for estimating fuel consumption. In our results, we observed the FCCS method to overestimate fuel load and fuel consumption compared to the ALS method. We think this is mostly a result of the different levels of spatial detail between approaches, since the ALS method captured more of the variability that exists in sparse forest and rangeland fuels than FCCS. Future efforts may be able to combine these approaches to better quantify fuel.

1. Introduction

Assessment of fire behavior, fire effects, and smoke are mutually important for wildfire management and planning (Prichard, Larkin, et al., 2019). Furthermore, characterization of pre-fire fuel loading is a critical measurement across these disciplines. Fuel load (the amount of live and dead fuel at a site) constrains fire behavior and subsequent fuel consumption along with fuel moisture and fire weather (Finney, 2001; Ottmar, 2014). Fuel

Resources: Andrew T. Hudak, Michael Billmire, Nancy H. F. French, Bridget Hass, Tristan Goulden

Software: T. Ryan McCarley, Michael Billmire

Supervision: Andrew T. Hudak, Nancy H. F. French, Roger D. Ottmar, Rainer Volkamer

Visualization: T. Ryan McCarley

Writing – original draft: T. Ryan McCarley

Writing – review & editing: T. Ryan McCarley, Andrew T. Hudak, Joseph C. Restaino, Michael Billmire, Nancy H. F. French, Roger D. Ottmar, Bridget Hass, Kyle Zarzana, Tristan Goulden, Rainer Volkamer

consumption, in turn, influences smoke emissions (Ottmar, 2014; Van Der Werf et al., 2017) and other fire effects across a burned landscape (Lentile et al., 2006).

Fuel loading and consumption are assessed in multiple ways, including in situ field measurements (e.g., Cansler et al., 2019; Lydersen et al., 2015), remote sensing from optical sensors or active sensors (e.g., García, Saatchi, Casas, Koltunov, Ustin, Ramirez, & Balzter, 2017; McCarley et al., 2020; Riaño et al., 2002) such as airborne laser scanning (ALS), and fuel classification systems which are developed through field-derived metrics and defined by the general vegetation of ecosystem type (Keane et al., 2013; Riccardi et al., 2007). Numerous equations have been derived to estimate canopy (E. D. Reinhardt & Crookston, 2003; E. Reinhardt et al., 2006), understory vegetation (Brown et al., 1982), and surface fuel (down woody debris, litter, and duff) loads (Brown et al., 1982; Woodall & Monleon, 2010) from field measurements. In rangeland ecosystems, destructive sampling within fixed micro-plots is an accurate approach to estimate fuel loading for small areas (Bonham, 1989; Marsett et al., 2006). Field data alone can provide estimates of fuel load on small scales; however, at coarser scales, integration with remote sensing or fuelbeds provides a more practical approach (Keane et al., 2013; Prichard, Kennedy, et al., 2019).

ALS data has demonstrated capabilities for estimating forest canopy fuels (Andersen et al., 2005; Riaño et al., 2003, 2004; Skowronski et al., 2011), forest surface fuels (Bright et al., 2017; Hudak et al., 2016; Jakubowski et al., 2013; Pesonen et al., 2008; Price & Gordon, 2016), and grassland and sagebrush steppe fuels (Jansen et al., 2019; A. Li et al., 2017). With ALS availability increasing, change detection using multitemporal ALS (i.e., the use of two or more ALS datasets across time at a given location) is also becoming more common. Other studies have used multitemporal ALS data to quantify fire-induced changes in fuel load (McCarley et al., 2020), fuel density (McCarley et al., 2020; Skowronski et al., 2020), fuel volume (Alonzo et al., 2017), and basal area (Hoe et al., 2018; Hu et al., 2019) in forests. To our knowledge, only Wang and Glenn (2009) have quantified fire-induced changes for a rangeland ecosystem using multitemporal ALS data, but they did not measure fuel load.

Many different fuel classification systems have been developed empirically from field data to characterize fuels and act as inputs for fire behavior and fire effects models (Keane et al., 2013; Riccardi et al., 2007). A central aspect of these systems is that they group and categorize the physical characteristics of fuels into components, or fuelbeds, that are functional from local to global scales. The Fuel Characteristic Classification System (FCCS) is one widely-used fuel classification system that was designed and applied across all ecosystems in the United States (Ottmar et al., 2007; Prichard et al., 2013; Riccardi et al., 2007). Within FCCS, structural variability is captured through the definition of fuelbeds in six horizontal strata, representing any scale of interest (McKenzie et al., 2007; Ottmar et al., 2007; Riccardi et al., 2007). FCCS was first compiled using published literature, fuels photo series, other fuel datasets, and expert opinion (Ottmar et al., 2007; Riccardi et al., 2007); however, others have employed the system world-wide using satellite Earth observation products and available field data (Pettinari & Chuvieco, 2016).

Within the United States, FCCS has been adapted for application within LANDFIRE (www.landfire.gov) program by the Fire and Environmental Research Applications team of the U.S. Forest Service Pacific Northwest Research Station. The 30 m LANDFIRE (hereafter LF) FCCS data is attributed with unique fuelbed ID's, representing specific fuel loading values for use in fire behavior and fire effects estimation. LF FCCS is used to estimate fuel loads at scales from a single fire (Campbell et al., 2007; French et al., 2011) to across the contiguous United States (F. Li et al., 2018). Additionally, these estimates can be used as an input for fuel consumption models such as CONSUME (Ottmar et al., 1993), which is accessible within Fuel and Fire Tools (FFT; Fire and Environmental Research Applications Team, 2020) software.

A limitation with FCCS is that a single fuel load value is used to estimate large areas of theoretically homogeneous or similar vegetation, while ignoring fine-scale heterogeneity at subpixel scales (i.e., <30 m). However, fuel loading fundamentally varies greatly at fine scales (Keane et al., 2013; Keane & Gray, 2013). Because variability is rarely incorporated into regional estimates of fuel load and consumption, it can be a notable source of uncertainty in fire behavior models (Cardil et al., 2021; Prichard, Kennedy, et al., 2019) or for deriving products such as carbon emissions (Chuvieco et al., 2019; French et al., 2004; García, Saatchi, Casas, Koltunov, Ustin, Ramirez, et al., 2017). Recent efforts have sought to quantify the uncertainties of fuel loading through the development of the North American Wildland Fuel Database (NAWFD; <http://nawfd.mtri.org>). The NAWFD was

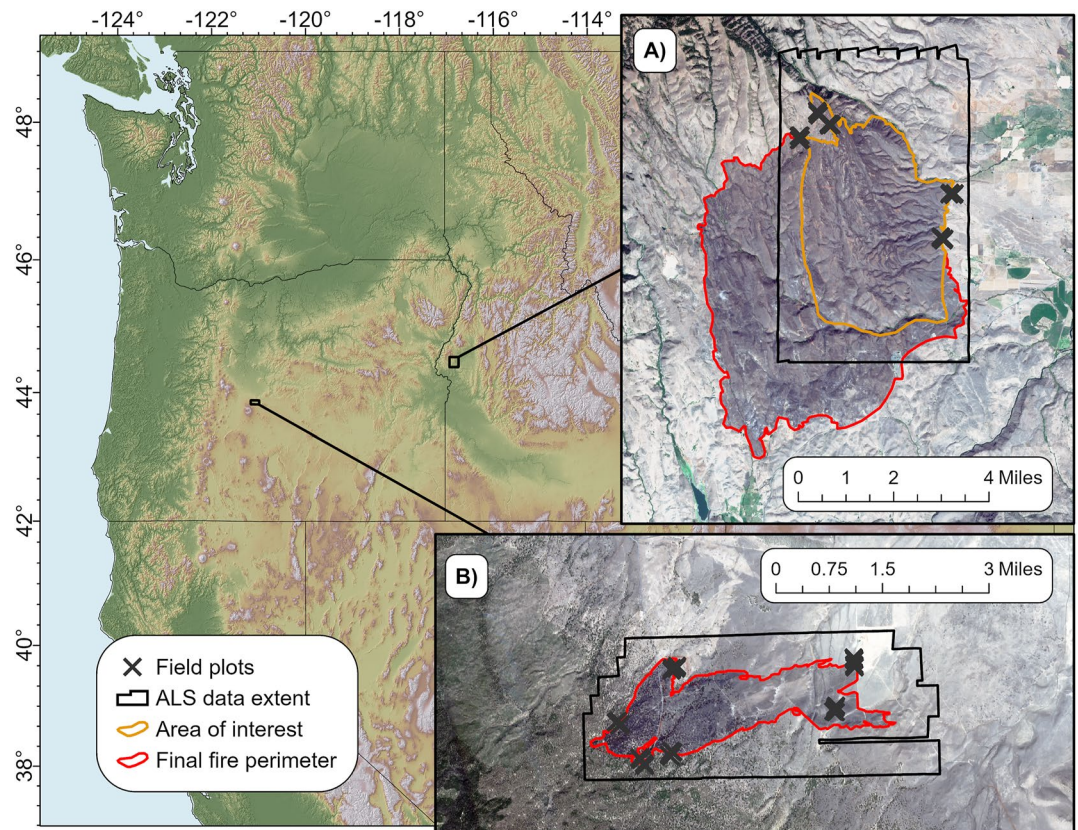


Figure 1. Location of Keithly (a) and Tepee (b) Fires, with field plot locations, post-fire ALS coverage extent, and fire perimeters. At the Keithly Fire, the ALS data were collected to evaluate an area of interest, the fire perimeter as of 26 July 2018, while at the Tepee Fire ALS data were available for the fire's maximum extent on 8 September 2018.

developed by matching over 26,620 field data records with LF Existing Vegetation Type (EVT) data in order to quantify the distribution of biomass estimates for any given EVT in the dataset (Prichard, Kennedy, et al., 2019). Subsequently, uncertainties for emissions derived from fuel loading have also been assessed, providing an understanding of the magnitude of uncertainty when using generalized fuelbed approaches (Kennedy et al., 2020). While these studies have sought to define the range of uncertainty, the errors stemming from fine-scale heterogeneity in fuels have not been explored at the scale of wildfire events that drive fire behavior and emissions.

Our main objectives for this study were to compare total fuel load and consumption estimates using the ALS and the FCCS approach for two wildfires and to determine the influence of fine-scale heterogeneity on the difference between ALS and FCCS fuel load and consumption estimates. Furthermore, the use of multitemporal ALS data to estimate fuel consumption in predominantly rangeland ecosystems is novel in this field. To achieve our objectives, we estimated total pre-fire fuel load (i.e., sum of the individual fuelbed categories) using ALS data (5 m resolution) trained with field data and LF FCCS data (30 m resolution). We estimated fuel consumption from the difference in pre- and post-fire ALS-estimated fuel load and by processing the FCCS data in CONSUME.

2. Materials and Methods

2.1. Study Area

We evaluated two fires which burned in 2018, the Keithly Fire (7,050 ha) and the Tepee Fire (794 ha) (Figure 1). The Keithly Fire occurred 20 km northeast of Weiser, Idaho, USA on hilly terrain dominated by sagebrush steppe and xeric grassland (Figure 2), with isolated pockets of Douglas-fir (*Pseudotsuga menziesii* (Mirb.) Franco) and tall shrub in the wetter drainages and steeper north-facing slopes. The Tepee Fire occurred 30 km southeast

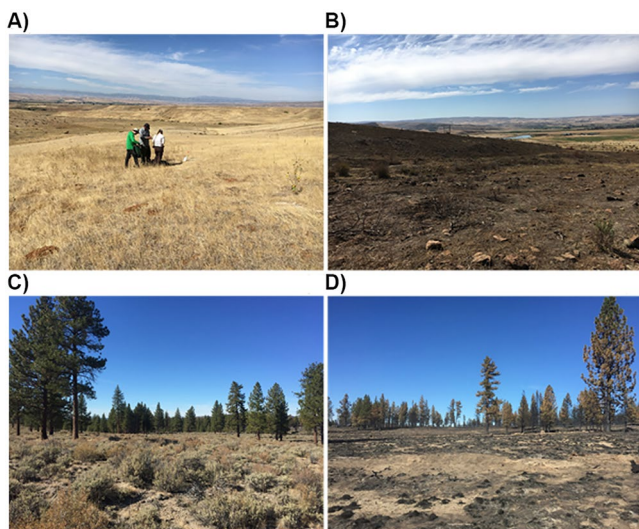


Figure 2. Typical unburned and burned fuels at the Keithly (top) and Tepee (bottom) Fires.

of Bend, Oregon, USA at the ecotone between sagebrush steppe and sparse ponderosa pine (*Pinus ponderosa* Dougl. Ex Laws.) Savanna, across mostly flat terrain (Figure 2).

2.2. Data Acquisition and Processing

2.2.1. Fire Perimeters

At both fires, the smoke plumes were sampled by a fixed-wing aircraft (King Air) as part of the Biomass Burning Fluxes of Trace Gases and Aerosols (BB-FLUX) Project (Volkamer et al., 2020). This limited post-fire ALS acquisition at Keithly to an area of interest corresponding to the fire perimeter on 26 July 2018 when the fire was at 2,947 ha (Figure 1). The fire continued to burn the next day before containment. At the Tepee Fire, plume sampling occurred on 8 September 2018, which was the only day of significant burning and when the fire reached near maximum size.

We obtained the 26 July 2018 fire perimeter for the Keithly fire and 8 September 2018 fire perimeter for the Tepee fire from the Geospatial Multi-Agency Coordination (GeoMAC) group. As of May 2020, the National Interagency Fire Center's National Incident Feature Service (<https://data-nifc.opendata.arcgis.com/>) managed these data. GeoMAC fire perimeters were based on thermal satellite data, which detect infrared heat at moderate resolution. Our

initial visual inspection showed that GeoMAC overestimated the fire perimeter at both fires. Therefore, we used post-fire Sentinel 2 multispectral satellite data to calculate the Mid-Infrared Bi-spectral Index (MIRBI; Trigg and Flasse, 2001), a burn-severity index previously demonstrated to provide high accuracy discernment between burned and unburned areas in similar rangeland (Sparks et al., 2015) and forest (McCarley et al., 2018) conditions. We then adjusted the outer burn perimeters manually in ArcGIS 10.6 (ESRI, Redlands, CA) using the MIRBI images as reference.

2.2.2. Field Plot Data

We collected field plot data in September and October of 2018 to capture post-fire conditions prior to regrowth of the vegetation. We identified locations for potential plots using LF 2014 FCCS to stratify for fuel conditions, after grouping similar FCCS classes; only FCCS classes comprising >10% of the burn area were targeted for sampling. While in the field, we randomly assigned actual plot locations to adjacent burned and unburned sites that had similar pre-fire structural conditions based on visual estimation. Because both fires were actively suppressed, field plots were located well clear of areas where fire retardant was dropped. We sampled a total of 66 plots in clusters of six. For each cluster, we installed three burned and three unburned plots inside and outside the fire perimeter respectively, with at least 30 m separation between plots (Figure S1 in Supporting Information S1). We recorded plot locations using a resource-grade Global Navigation Satellite System receiver (Geo7X, Trimble Inc.) with real-time differential correction, and applied post-processing corrections for added accuracy. Mean post-processed horizontal accuracy was 0.19 m with a standard deviation of 0.12 m.

Plot sampling protocol was slightly different for rangeland ($n = 48$) and forested ($n = 18$) areas. In rangeland plots, we placed a 1 m² quadrat at plot center in line with the other plots in the series. All vegetation, surface woody, and ground fuels were separated by type and destructively harvested to be oven dried and weighed in the laboratory. Collected fuel types included litter (including any small down woody debris), herbaceous vegetation (grasses and forbs), and shrubs separated into 0.5 m vertical strata. We followed the same procedure for forested plots with a few additions. We measured down woody debris, litter, and duff along a 15 m transect oriented perpendicular to the prevailing slope and centered on the plot, and calculated biomass as described in Brown et al. (1982). We measured the 1000-hr and 100-hr fuels along the entire transect and measured litter and duff depths at 0, 6, 9, and 15 m along the transect. We collected, oven-dried, and weighed 10-hr and 1-hr fuels within the quadrat at plot center. We measured tree height, dbh, and live or dead status for all trees and saplings (less than 12 cm dbh) within 5.6 m of plot center and for additional trees between 5.6 and 8 m of plot center. We also recorded height to live crown and crown base height for all trees. Biomass (tree boles, snags, and crown material) was calculated using the Fire and Fuels Extension of the Forest Vegetation Simulator (E. D. Reinhardt & Crookston, 2003).

Table 1
Characteristics of Pre- and Post-Fire ALS Acquisition Parameters

	Tepee Fire		Keithly Fire	
	7–8 September 2018		25–27 July 2018	
Acquisition year(s)	2010; 2011	2018	2017	2018
Date(s) of acquisition	6–13 September; 31 July to 10 August	18 September	14–27 September	6 September
ALS system	Leica ALS60	Riegl Q780	Leica ALS80	Riegl Q780
Flight altitude	1,300 m	1,000 m	1,800 m	1,000 m
Swath overlap	50%	37.2%	64%	50%
Point density	9.4 p/m ²	7.1 p/m ²	4.9 p/m ²	8.9 p/m ²
First return density	9.0 p/m ²	6.1 p/m ²	4.8 p/m ²	8.3 p/m ²
Scan frequency	52 Hz	102 Hz	48 Hz	102 Hz
Scan angle	±14°	±18.5°	±20°	±18.5°

2.2.3. ALS Data

Repeat ALS data were available for both fires (Table 1). Pre-fire ALS data for the Keithly Fire were collected in 2017, while pre-fire ALS data for the Tepee Fire were comprised of two collections from 2010 and 2011 (Figure S2 in Supporting Information S1). At both fires, the National Ecological Observatory Network (NEON) collected post-fire ALS shortly after the fires and close to the time of field data collection in 2018. The extent of the post-fire ALS acquisitions was designed to match the BB-FLUX project areas. The total area of repeat ALS data was 6,686 ha at the Keithly Fire and 2,396 ha at the Tepee Fire. Differences in the ALS acquisitions such as, low ALS point density in the pre-fire data at Keithly, the long time between pre- and post-fire ALS data at Tepee, sensors used, and flight parameters likely contributed to uncertainty in the results; however, these were the only data available.

Ground returns for all ALS data collections were classified using the ‘lidR’ package in R (Roussel & Auty, 2019) with a progressive morphological filter (Zhang et al., 2003) to better distinguish low vegetation. The remaining ALS data processing was conducted in LAStools (Isenburg, 2013). ALS point clouds were height normalized, gridded to 5 m rasters, and statistical metrics were calculated for each raster cell. We used only first returns to produce metrics, as we observed this to yield more comparable metrics from near-ground returns and compensate for the relatively lower point density in the pre-fire Keithly data. We removed outliers below –30 m and above 150 m of the DEM, following Forest Service procedure (*pers. comm.* R. McGaughey, USFS). We generated over-story canopy metrics with a height return cutoff of 2 m. We calculated identical statistical metrics for the point cloud at each plot location but using a different selection radius for rangeland and forested plots. ALS points were clipped to a 3 m radius rangeland plots, following Hudak et al. (2016). An 8 m radius was used to clip ALS points at forested plots to match the maximum sampling radius used in the field data collection. We used plot metrics for fuel model training, while gridded metrics (5 m resolution) were used to apply models and generate fuel maps across the landscape.

We used post-fire field data and post-fire ALS data clipped to the plots to model the relationship between total fuel load (Mg ha⁻¹) and the point cloud height and density metrics. We then applied the model to both pre- and post-fire gridded ALS metrics to map fuel and estimate consumption. Modeling was done using the Random Forest (RF) algorithm (Breiman, 2001), but first we evaluated and then selected model variables from a large candidate pool by testing for high correlation (Pearson’s $r > 0.9$) and multi-collinearity using a Gram-Schmidt QR-decomposition approach. For the model to achieve optimal fit, while remaining parsimonious, the Model Improvement Ratio (MIR; Murphy et al., 2010) was employed from the “rfUtilities” (version 2.1–5) R package (Evans & Murphy, 2017) to select the final ALS metrics (Table 2) from those initially selected. MIR scores are calculated as the importance of a given variable (a statistic given in RF) divided by the maximum model

Table 2
ALS Metrics of Vegetation Structure Selected by Model

ALS metric	Statistic of the ALS point cloud
PCT 0–0.5 m	Percent of first returns ≤0.5 m
PCT 2–4 m	Percent of first returns >2 m and ≤4 m
PCT 16–32 m	Percent of first returns >16 m and ≤32 m
COV	Percent of first returns ≥2 m
P75	75th percentile of the height values for first returns
P95	95th percentile of the height values for first returns

importance including all variables. The process for using MIR in variable selection, described in greater detail in Murphy et al. (2010), is an iteration of computing MIR scores through the available variables until a set is found that minimize model mean squared error and maximize percent variance explained. Random forest modeling and the MIR procedure are further described in McCarley et al., 2020, but are also based on other studies that have estimated fuel load using ALS data in forested ecosystems (Bright et al., 2017; Fekety et al., 2015; Hudak et al., 2012), rangeland (Jansen et al., 2019; A. Li et al., 2017), and other shrublands (Greaves et al., 2016).

Accurate change detection through the differencing of two ALS datasets is contingent on the assumption that fire is the only major process occurring on the landscape between ALS acquisitions. However, this is rarely the case. At the Keithly fire, 96% of the burn perimeter fell within Bureau of Land Management grazing allotments (https://gis.blm.gov/arcgis/rest/services/range/BLM_Natl_Grazing_Allotment/MapServer), which means some of the change in fuel load may be attributed to herbivory and not wildfire. We could not quantitatively test how much fuel load change was due to grazing and we could not exclude the areas because they represent a vast majority of the fire. Thus, changes due to herbivory are unaccounted for in the results and contributed to the overall uncertainty. At the Tepee fire, there was less evidence of grazing, but there were forest management activities accounted for using the US Forest Service Forest Activity Tracking System (FACTS; USDA Forest Service, 2020). An area of 250 ha within the ALS acquisitions, west of the fire, was subjected to precommercial thinning, commercial thinning, and prescribed burning between 2010 and 2018 (Figure S3 in Supporting Information S1). These treatments included a only a small portion of the fire (19 ha), which was subsequently excluded from the analysis because estimated change could be due to management and not wildfire.

2.2.4. FCCS Data

For both fires, we obtained FCCS fuelbeds from the LF 2016 remap, which was the closest LF FCCS fuelbed mapping to the pre-fire conditions. We used all FCCS classes, even if we did not observe the listed vegetation types in the field, since many FCCS users do not have the ability of ground-truthing the fuelbeds. The LF 2016 remap includes codes to account for disturbances such as wildfire, fuel and vegetation treatments, insect and disease, storm damage, and invasive plants. At the Keithly Fire, 5.5% of the LF data within the fire perimeter had disturbance codes for the 2012 Roadside Fire. However, the LF 2016 remap had already accounted for the previous fire, as those areas were mostly classified as introduced grasses. At the Tepee fire, 1.7% of the LF data within the fire perimeter had disturbance codes for fuel treatments. These areas were accounted for by masking out fuel treatments using FACTS.

We downloaded FFT (version 2.0.2017) from the University of Washington FFT site (<https://depts.washington.edu/fft/>). We calculated pre-fire fuel load for each LF FCCS class by running the FCCS Fuel Characteristics Calculator (version 4.0.999) from an executable Java application included in the FFT download. To estimate fuel consumption, we implemented the FFT version of CONSUME (version 5.0) in Python (see Text S1 Supporting Information S1). Environmental fuel conditions in CONSUME were set based on expert opinion (*pers. comm.* R. Ottmar, USFS). Finally, we assigned pre-fire fuel load and fuel consumption estimates to their corresponding LF FCCS fuelbed class in raster format to map the predictions.

2.3. Data Analysis

To compare fuel load and consumption estimates using the ALS and the FCCS approach for each fire, the 30 m LF FCCS were first re-projected and resampled to match the 5 m ALS data. We calculated fuel load (Mg ha^{-1}) estimates from the mapped data, using the 26 July 2018 fire perimeter at the Keithly Fire and the 8 September 2018 fire perimeter at the Tepee Fire (Figure 1).

Although much of the area at both fires was composed of rangeland, forest represented the largest source of biomass. Individual and sparse stands of trees dotting the landscape represents high fine-scale variability in biomass, which the ALS data more easily captured than LF FCCS. To diagnose the impact of spatial scale between the two approaches, this study partitioned: (a) areas where FCCS classes included tree biomass, but there were no trees (i.e., false positive); (b) areas where FCCS classes did not include tree biomass, but there were trees (i.e., false negative); and (c) areas where FCCS classes correctly included or did not include tree biomass (i.e., true positive/negative or areas in agreement). We used LF EVT data to partition FCCS classes that included tree biomass, while also preserving some major differences in vegetation type. We included only the most common EVTs, and choose to group rare EVTs into more common ones (Figure S4 in Supporting Information S1). Each

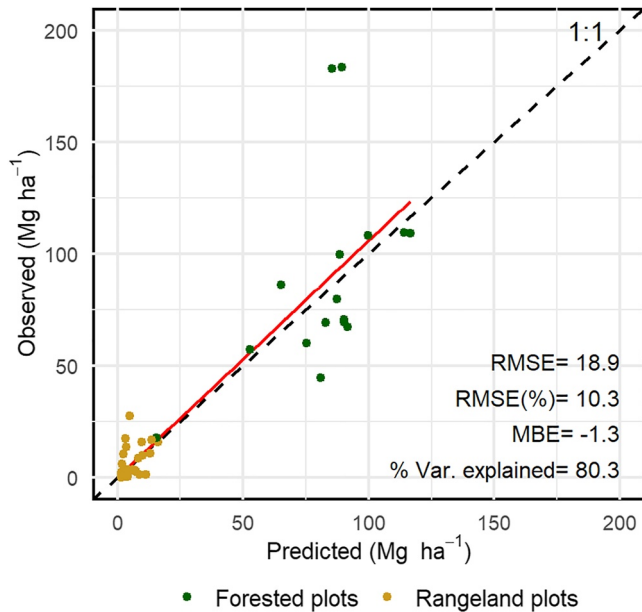


Figure 3. Performance statistics for the RF model of ALS metrics and field data, with one-to-one line (dashed) and the line of best fit (solid). Plots with tree measurements (forested plots) and without (rangeland plots) are distinguished.

fire was further partitioned into areas of likely forest or non-forest based on whether any ALS returns were observed higher than 2 m above the ground. Using these designations, comparisons of the ALS and FCCS approach were made in areas of agreement (i.e., both FCCS and ALS data includes trees or not), areas of false positives (i.e., FCCS shows trees, ALS does not), and areas of false negatives (i.e., FCCS shows no trees, ALS does).

Neither the ALS data nor the LF data represented “true” ground conditions and field data was not independent from the ALS models. Therefore, we used data from NAWFD to approximate the uncertainty in biomass values for each EVT group and provide an independent reference data set for the estimates in this study. We calculated NAWFD fuel consumption estimates in CONSUME following the same procedure as the LF FCCS fuelbeds.

3. Results

The RF model developed for predicting fuel load from post-fire ALS metrics performed well, explaining 80.3% of the variance between predicted and observed values. Additionally, the regression line closely aligned with the 1:1 line (Figure 3), and root mean squared error (RMSE) was low. The model had a slightly negative mean bias error (MBE), calculated as the mean of the predicted values minus the observed values. This bias was largely driven by two notable outliers in model, where predicted fuel load was on average 96 Mg ha^{-1} less than observed fuel load. Both outlier sites were unburned forested plots at the Tepee Fire.

We mapped pre-fire fuel load and fuel consumption using the FCCS and ALS approaches for the Keithly (Figure 4) and Tepee (Figure 5) fires. Visually, the maps indicated that both approaches estimated higher fuel load and consumption in forested areas than rangeland areas, but that the ALS data captured more variation in fuel load and consumption due to higher spatial resolution. The FCCS estimates appeared to have greater fuel load and consumption than the ALS estimates.

Quantitatively, pre-fire fuel load and fuel consumption were higher using the FCCS approach than the ALS approach (Figure 6). At the Keithly Fire, the FCCS-derived pre-fire fuel load was $34,175 \text{ Mg}$ (103%) higher than the ALS-derived estimate. The FCCS fuel consumption estimate was $27,631 \text{ Mg}$ (213%) higher. For the Tepee Fire, FCCS estimates were higher than ALS estimates by $19,979 \text{ Mg}$ (74%) for pre-fire fuel and $3,213$ (28%) for fuel consumption. Using FCCS, we estimated 60% of the pre-fire fuel was consumed at the Keithly Fire, while 31% was consumed at the Tepee Fire. Using ALS, we estimated 39% of pre-fire fuel was consumed at the Keithly Fire and 42% at the Tepee Fire.

Pixels in major EVTs with a tree component, but without any ALS returns above 2 m (i.e., false positives) accounted for some of the difference in estimated pre-fire fuel load. The Ponderosa savanna EVT comprised most of this area and showed the biggest differences (Figure 7). We attributed an additional $6,334 \text{ Mg}$ (108.8 Mg ha^{-1}) for the Keithly Fire and $15,507 \text{ Mg}$ (176.5 Mg ha^{-1}) for the Tepee Fire to false positives, approximating the overestimation of pre-fire fuel by the FCCS approach in areas that are classified as having trees, but don't. For false negatives, pixels in EVTs without a tree component and having ALS returns above 2 m, ALS estimates were higher than FCCS estimates by $3,543 \text{ Mg}$ (23.7 Mg ha^{-1}) at Keithly and $5,517 \text{ Mg}$ (71.8 Mg ha^{-1}) at Tepee. Taken together, the net overestimation of the FCCS approach attributed to heterogeneity in the forest-rangeland ecotone was $2,791 \text{ Mg}$ at Keithly and $9,990 \text{ Mg}$ at Tepee, representing 8.2% and 50.0% of the observed difference in total fuel between approaches.

The overestimation of trees in FCCS at the Tepee Fire was considerable, yet a majority of the difference between approaches was not caused by misclassification between forest and rangeland. Instead, areas in agreement (Figure 7) accounted for 91.8% of the difference in pre-fire fuel load between approaches at the Keithly Fire and 50.0% of the difference at the Tepee Fire. At Keithly, there was a notable difference in estimates for big sagebrush and deciduous shrubland EVT classes; however, both FCCS and ALS estimates were within the interquartile

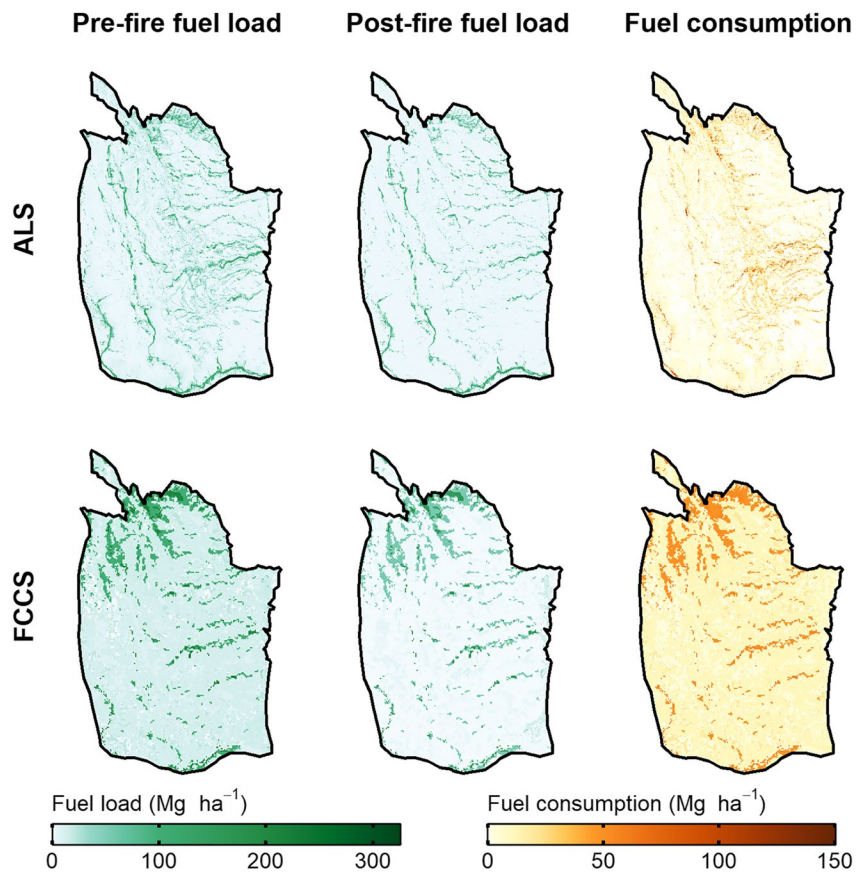


Figure 4. Fuel load and consumption estimated for the Keithly Fire.

range of NAWFD data, showing that a wide range of fuel loads had been observed for those EVT in other field studies. Meanwhile, the FCCS estimates for Ponderosa Savanna were higher than both the ALS estimates and the NAWFD 75th percentile for both fires.

The differences in fuel consumption between the FCCS and ALS approaches (Figure 8) displayed similar trends to fuel load. For pixels in EVT with a tree component that did not have ALS returns above 2 m (i.e., false positives), FCCS estimates were 1,396 Mg (24.0 Mg ha⁻¹) higher at Keithly and 3,383 Mg (38.5 Mg ha⁻¹) higher at

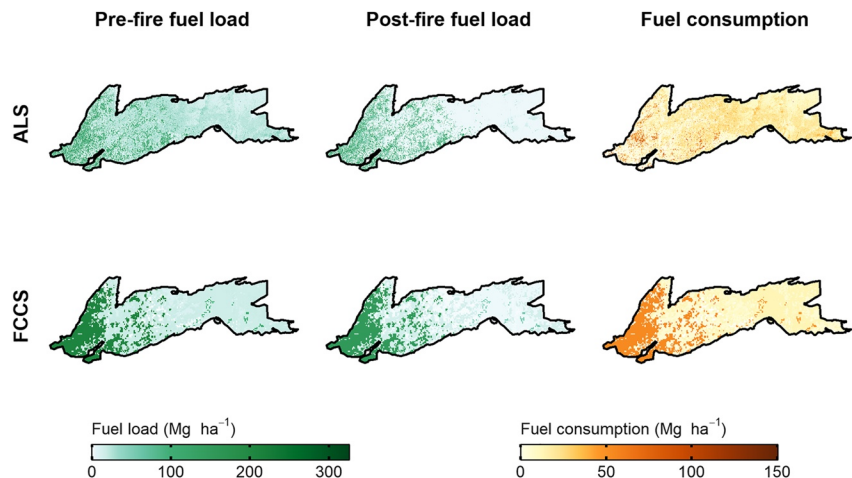


Figure 5. Fuel load and consumption estimated for the Tepee Fire.

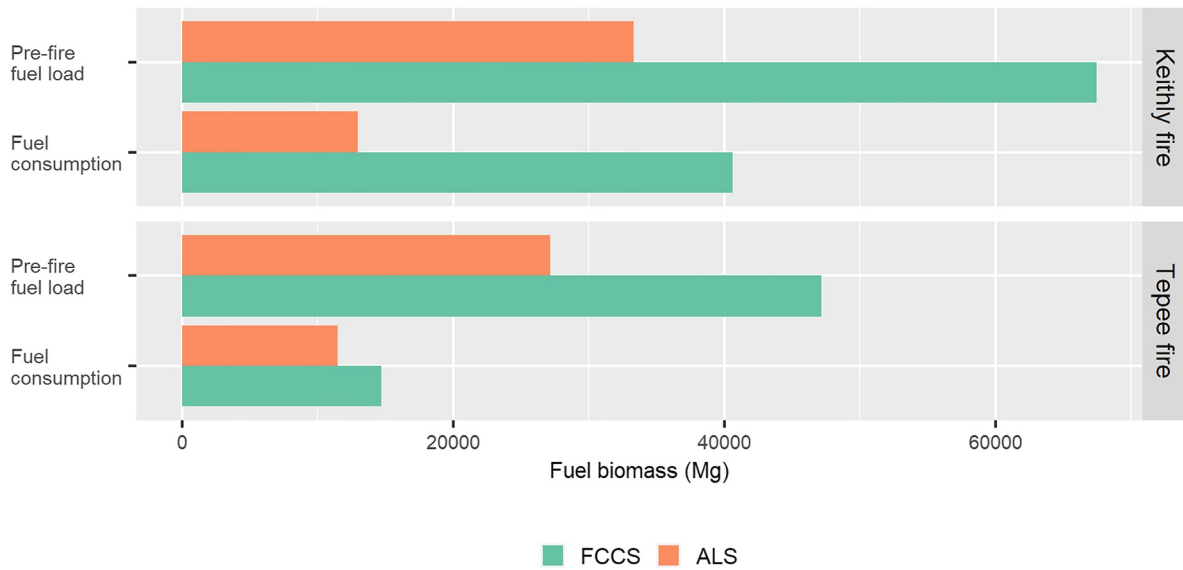


Figure 6. Estimated pre-fire fuel load and fuel consumption for the Keithly and Tepee fires.

Tepee. For false negatives, FCCS estimates were 979 Mg (6.5 Mg ha^{-1}) higher at the Keithly Fire, but 577 Mg (7.5 Mg ha^{-1}) lower at the Tepee Fire, resulting in overestimation of 2,375 and 2,806 (8.6% and 87.3% of the difference in estimated consumption).

For pixels in agreement, ALS estimates were generally lower than FCCS estimates and tended to be at or below the 25th percentile of the NAWFD data. Although, at the Tepee Fire, we observed greater consumption from ALS than FCCS within the big sagebrush EVT. Areas in agreement (Figure 7) accounted for 91.4% of the difference in fuel consumption between approaches at the Keithly Fire and 12.7% of the difference at the Tepee Fire.

4. Discussion

We consistently estimated higher pre-fire fuel load and fuel consumption using the FCCS approach than the ALS approach at both fires. The difference in fuel load and fuel consumption between the two approaches can be explained by a few factors. First, bias in the RF model (Figure 3) suggests that the ALS approach may be underestimating fuel load. Second, the ALS data (5 m resolution) captured forest heterogeneity at a smaller scale than the resolution of LF FCCS (30 m), which led to considerable FCCS false positives (i.e., areas where FCCS classes included tree biomass, but there were no trees) at the Tepee Fire and to a lesser extent the Keithly Fire (Figures 7 and 8). Finally, by providing continuous biomass estimates rather than discrete values, the ALS approach is more sensitive to variation in fuel load and consumption (Figures 4 and 5), which over large areas could explain much of the difference we observed between approaches. These ideas are discussed further in the following sections.

4.1. ALS Approach

Uncertainty in the RF models likely propagated some error into the fuel load and consumption estimates from ALS data. Model bias showed the RF model underestimated fuel load by an average of 1.3 Mg ha^{-1} . This equates to an additional pre-fire fuel load of 3,831 Mg at Keithly and 1,032 Mg at Tepee, although this accounts for only a fraction of the difference between the ALS and FCCS estimates. Most of the predictions in the model had a close one-to-one relationship with observed fuel load (Figure 3); however, the two field plots with the highest observed fuel load had 182.8 Mg ha^{-1} and 183.6 Mg ha^{-1} but were predicted to be 85.3 Mg ha^{-1} and 89.3 Mg ha^{-1} . These sites also had the highest tree biomass but were starkly different in structure. The first plot had only two large diameter trees, while we recorded only 23 trees in the other plot (average number of trees for the forested plots was 3.7). Litter and duff composed 25% and 34% of total fuels at the two field plots with the highest observed

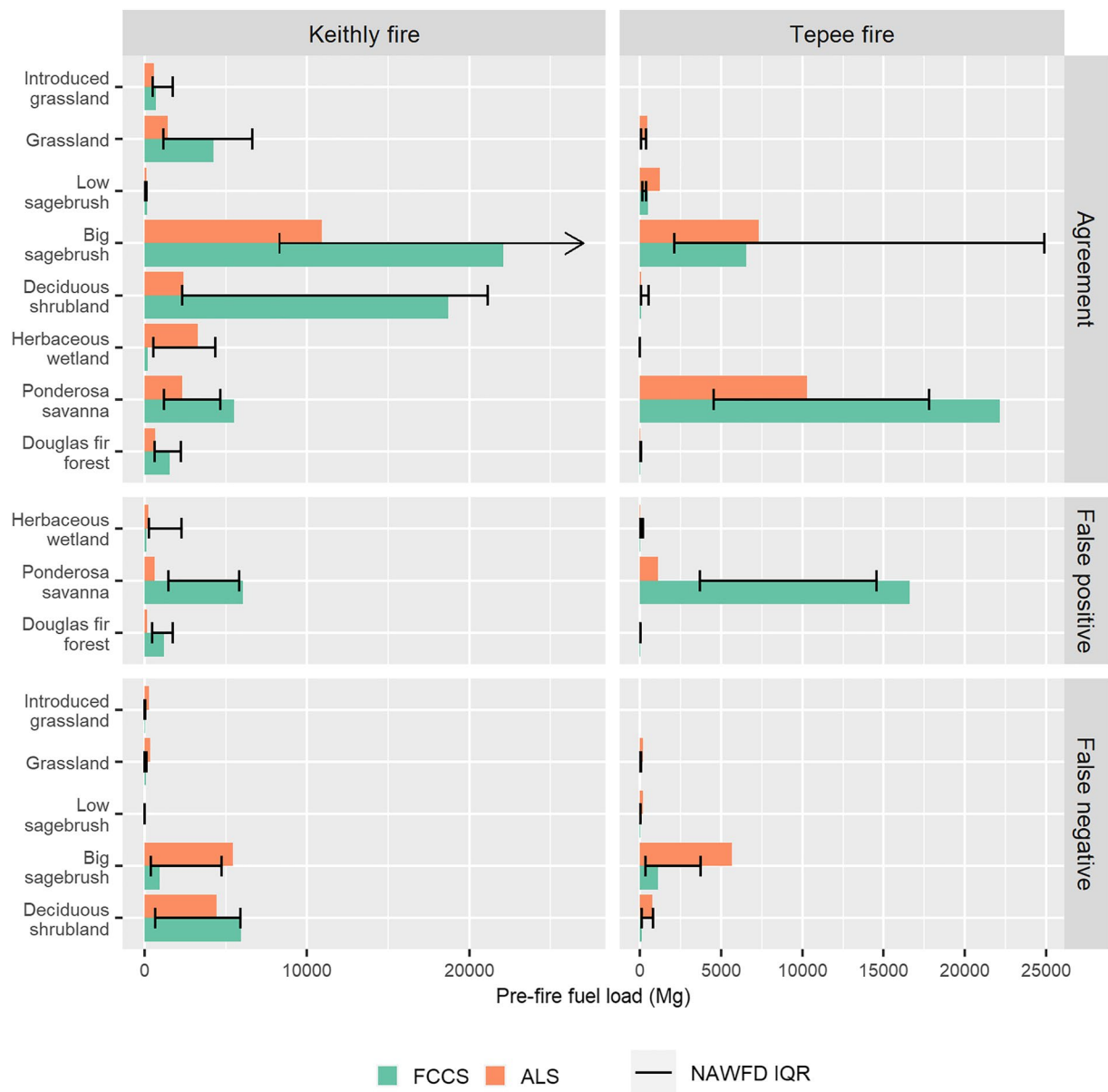


Figure 7. Pre-fire fuel load estimated from FCCS and from ALS within the dominant EVT classes. Also shown are the 25th and 75th percentile loadings from NAWFD for each EVT class. The NAWFD 75th percentile for Big Sagebrush at the Keithly Fire (indicated by the arrow to exceed the x-axis) was 110,760 Mg. False positives are areas where FCCS classes included tree biomass, but there were no trees, false negatives are areas where FCCS classes did not include tree biomass, but there were trees, and areas of agreement are where FCCS classes correctly included or did not include tree biomass.

fuel loads but was as much as 76% of fuel at one plot which had 7.2 Mg ha⁻¹ of litter and 74.8 Mg ha⁻¹ of duff. At this site, we measured 108.2 Mg ha⁻¹ of total fuel, while RF predicted 99.9 Mg ha⁻¹. Two plots may have vastly different number and size of trees but be within 1 Mg ha⁻¹ of biomass, as was the case with the outliers here. These issues highlight the difficult task being performed by RF and the need for sufficient training data to characterize the complex relationship between structure and biomass. Field observations in this study were heavily skewed toward lower plot biomass (Figure S5 in Supporting Information S1), which likely contributed to underestimation of higher biomass plot as fewer training points were available for the RF model to characterize structural differences in higher productivity sites.

The inclusion of surface fuels is also complicated, as some plots had considerable litter and duff loads (Figure S6 in Supporting Information S1), which are not directly detected by ALS. Therefore, ALS fuel models must rely

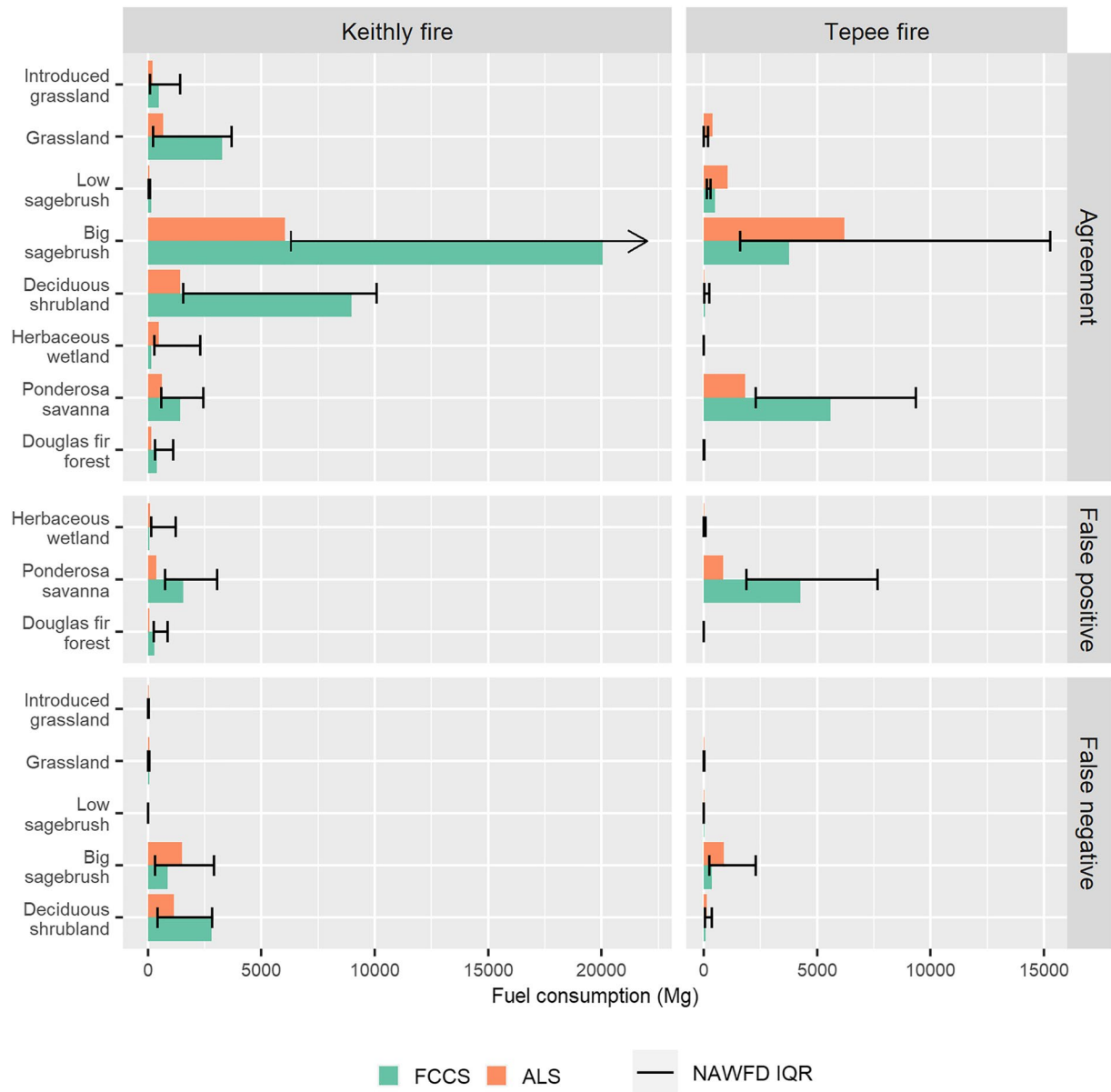


Figure 8. Average fuel consumption estimated using CONSUME from FCCS and from ALS within the dominant EVT classes. Also shown are the 25th and 75th percentile loadings from NAWFD for each EVT class. The NAWFD 75th percentile for Big Sagebrush at the Keithly Fire (indicated by the arrow to exceed the x-axis) was 67,925 Mg. False positives are areas where FCCS classes included tree biomass, but there were no trees, false negatives are areas where FCCS classes did not include tree biomass, but there were trees, and areas of agreement are where FCCS classes correctly included or did not include tree biomass.

on the assumption that the overlying vegetation structure covaries with nondetectable strata, for example, more trees should result in more underlying litter and duff. Other studies have explored this topic at field sites and found that while overstory characteristics are often correlated with surface fuels, the relationships are weakened by inherent fuel heterogeneity and can be different depending on overstory species (Cansler et al., 2019; Lydersen et al., 2015). This study did not attempt to distinguish tree species; however, we only observed ponderosa pine at the Tepee fire. Thus uncertainty in the estimation of the surface fuel component stems mostly from the unpredictability of the relationship between the overstory and understory.

The performance of the model in this study ($r^2 = 0.80$, RMSE = 10.3%, MBE = -1.3 Mg ha^{-1}), was similar to results from McCarley et al. (2020; $r^2 = 0.68$, RMSE = 10.85%, MBE = -0.03 Mg ha^{-1}), which modeled fuel load using ALS data and 216 field plots from two fires. Additionally, Hudak et al. (2012), Fekety et al. (2015),

and Zhao et al. (2018) each achieved comparable or higher r -squared values (0.75–0.92) from their models in forested ecosystems. Fewer studies have quantified fuel load from ALS data in rangeland ecosystems, which was the primary land cover type of both fires. Both Jansen et al. (2019; $r^2 = 0.64$, $MBE = -0.097 \text{ Mg ha}^{-1}$) and A. Li et al. (2017; $r^2 = 0.80$, $MBE = -0.072 \text{ Mg ha}^{-1}$) achieved rangeland biomass models with much less bias. There is considerable difficulty distinguishing the ground surface with short grasses and low sagebrush (Spaete et al., 2011), which presents challenges normally not encountered in forested ecosystems. Both Jansen et al. (2019) and A. Li et al. (2017) employed different methods to separate and classify ground and vegetation points, which may explain some difference in model performance. However, the bias in this study was also largely driven by forested plots, which were not modeled by Jansen et al. (2019) or A. Li et al. (2017) and have naturally higher fuel densities and thus higher potential for cumulative bias.

4.2. FCCS Approach

Due to its finer resolution, the ALS data captured greater spatial detail of pre-fire fuel loads and subsequently more nuanced change in fuel load, including areas within the fire perimeter that may have been untouched by fire. At both these fires, forested areas were predominantly open, with ample spacing between trees. The 5 m ALS metrics easily distinguished this spatial arrangement, but in the 30 m LF FCCS data it was poorly differentiated, leading to considerable overestimation of pre-fire fuel by the FCCS approach. We observed this pattern in portions of the Keithly Fire, but because there were far fewer forested pixels the cumulative bias was not as prominent, accounting for only 8.2% of the difference between the FCCS and ALS approaches in estimating pre-fire fuel and 8.6% estimating fuel consumption. Instead, this was most evident for the Tepee fire, where LF pixels classified as forested fuelbeds were a mix of forest and non-forest, given that the fire spanned the ecotone between sagebrush steppe and ponderosa pine savanna. Here, 49.7% of the difference in pre-fire fuel estimates and 82.3% of the difference in fuel consumption estimates originated in FCCS forest fuelbeds in non-forested pixels.

FCCS approximates the mean of a given fuelbed, to be widely applicable. Yet, being at the ecotone, the forest observed at the Tepee Fire was on the lower end of productivity. Plot data showed that average fuel load for forested plots was 88.4 Mg ha^{-1} , whereas Pacific ponderosa pine forest, the dominant FCCS class in those areas, is reported to have 207.3 Mg ha^{-1} . It is possible that a more homogenous ponderosa pine forest would be in better agreement with this FCCS estimate. However, another issue is that automatically classified FCCS maps, such as LF, often contain errors. This study used the most recent pre-fire LF FCCS (2016), but the previous version (2014) had much of the forest at the Tepee Fire classified as Ponderosa pine savanna rather than Pacific ponderosa pine. The former FCCS class is reported to have 98.0 Mg ha^{-1} , a figure much closer to what was observed in the field data. There were a number of other FCCS classes present which listed vegetation species not present at these sites, such as Mesquite savanna. This study specifically did not attempt to correct any of the LF FCCS data that appeared erroneous, because it is unlikely that most LF users would perform such adjustments and it was important to assess LF FCCS as an off-the-shelf product.

The largest difference between the ALS and FCCS approaches at the Keithly Fire were in the big sagebrush and deciduous shrubland EVTs, even when we accounted for trees. This suggests that the spatial heterogeneity within rangeland environments is also a significant contributor of error. Furthermore, the big sagebrush EVT was present at both fires, but differed considerably in fuel load and consumption. At the Tepee fire the big sagebrush EVT was at the high end of the productivity gradient, bordering on ponderosa pine savanna, whereas sagebrush fuel densities at the Keithly Fire were at the opposite end of the gradient (Figure 2). Average ALS estimate fuel load for pixels in big sagebrush, with no returns above 2 m, was 5.7 Mg ha^{-1} at Keithly and 17.0 Mg ha^{-1} at Tepee. The FCCS averages, 11.6 Mg ha^{-1} and 15.5 Mg ha^{-1} , were more similar as they were composed of similar FCCS classes. We did not observe sagebrush to exceed 2 m in height in the field.

Other studies have demonstrated similar issues validating LF FCCS with finer-scale fuel measurements. Analyzing much of the western United States, Keane et al. (2013) found that fuel loading of duff, litter, and woody debris mapped in LF refresh 2008 FCCS was poorly correlated to those measurements in field plots. However, as McKenzie et al. (2007) noted, validating coarse FCCS data with finer-scale data can be misleading because the processes observed are dependent on the scale of analysis. FCCS fuelbeds could be generated at a finer scale than what is available through LF, which would help capture more heterogeneity in fuels. After all, LF FCCS is not designed to estimate fuel heterogeneity at less than 30 m and its development was instead focused on consistent,

comprehensive yet categorical fuelbed type mapping to be used across landscapes and management boundaries (Rollins, 2009). However, there is always a trade-off between generating products at finer-scale and maintaining generality.

The LF FCCS approach likely also overestimated fuel consumption. This was partly due to the overestimation of forested fuels, which yield more consumption in CONSUME, but also due to the parameters assigned to the model, including the fire perimeter. The FCCS approach assigns all areas within the fire perimeter a fuel consumption estimate. Thus, unburned islands would incorrectly contribute to fuel consumption, leading to overestimation. Furthermore, since FCCS is a discrete classification system, the CONSUME outputs are not sensitive to variability in fire severity, meaning overestimation would also occur in areas of lower fire severity. With the ALS approach, fuel load and consumption are continuous variables, meaning that some areas had no consumption or even small amounts of growth, particularly outside the fire perimeter.

4.3. Fusion of ALS and FCCS

The goal of comparisons such as this should not be to denigrate the respective approaches that differ in scale and purpose by design, but instead to understand their limitations and find opportunities for synergy. Although we could improve the RF models with more training data in high biomass areas, they still demonstrated greater sensitivity to fine-scale heterogeneity than the LF FCCS data. The clear advantage of LF FCCS is that it can be employed easily across the contiguous United States, without requiring existing ALS data or the cost associated with acquiring new ALS acquisitions. The LF FCCS approach produced pre-fire fuel load estimates within or near the interquartile range of NAWFD observations once we removed the misclassified (false positive and false negative) areas. This suggests that including the uncertainty of estimates, as described by Prichard, Kennedy, et al. (2019) and Kennedy et al. (2020), may be sufficient to describe emissions over large areas and multiple fires. However, there is also opportunity for improvement through fusion with ALS data or other sources.

Currently, LF FCCS classifies fuelbeds using products derived from topography, biophysical gradients, and Landsat imagery (Rollins, 2009). However, fuels in similar biophysical settings and with similar optical reflectance can vary in height, leading to misclassification errors (Riaño et al., 2002). Additionally, as we observed in this study, ecotones present a classification challenge, as a given pixel might not fully represent either ecosystem. In these cases, integration between FCCS and ALS could reduce the uncertainty of estimates, as ALS and other lidar systems can more accurately measure vegetation height. This could help improve classification accuracy, but also provide continuous variable data for adjusting fuelbed values in ecotones or other areas that aren't well-defined in FCCS. Such adjustments do not necessarily need to be incorporated in the LF FCCS program but could instead be performed retroactively using available lidar data. At coarse-scales (1 km), spaceborne lidar has been used to map forest canopy height (Simard et al., 2011), which was used by Pettinari and Chuvieco (2016) to produce global FCCS fuel data. Spaceborne lidar has also been used in conjunction with Landsat imagery to estimate existing biomass in a rangeland ecosystem similar to fires in this study (Glenn et al., 2016). ALS data have been used similarly in forested ecosystems (García et al., 2011; Jakubowski et al., 2013). At fine-scales (<1 m), terrestrial lidar has been effective at quantifying fuel heterogeneity (Hiers et al., 2009) and consumption (Hudak et al., 2020), which may prove useful to verify and refine sub-meter FCCS fuelbed characteristics. This study showed that, at the Tepee Fire, 50.0% of the difference in fuel load and 87.3% of the difference in fuel consumption was related to poor distinction of trees at the forest-rangeland ecotone. Thus while enhanced quantification of fine-scale fuel variable would be beneficial for improving fuel estimates in all ecosystems, the benefit may be more apparent in highly heterogeneous places.

Vegetation height alone is sometimes insufficient to improve fuel estimates. At the Keithly fire, overestimation of tree biomass was a minor contributor (<10%) to the difference between FCCS and ALS estimates. Fuel strata that don't vary in height (i.e., litter and duff) also confound these estimates. Here, other data sources such as hyperspectral imagery might be used in conjunction with ALS data to better distinguish rangeland fuelbeds and provide sub-meter estimates of surface fuel (Mundt et al., 2006). Post-fire data collected by NEON at both fires included high resolution (1 m) hyperspectral imagery that could be used for improved fuel speciation in the future. Currently, refinement of FCCS using methods such as ALS or hyperspectral imagery will be impractical for regional assessments, spanning multiple fires. However, at the scale of individual fires like those in this study, there are numerous opportunities to improve fuel load and consumption estimates.

5. Conclusion

Comparison of fuel load and consumption estimated at different scales can provide insight into the sensitivity of the alternative estimates of spatial fuel variability (Prichard, Kennedy, et al., 2019). The categorical LF FCCS fuel load estimates, designed to be representative at regional to national scales, overestimated fuel load and consumption at these two wildfire events, likely situated in fuel conditions that differed from mean fuelbed conditions for the mapped FCCS fuelbed types. Maps derived from local field and ALS datasets worked well at capturing fine-scale variation at 5 m resolution, 6× higher than the LF FCCS map scale (30 m). This proved to be important for distinguishing tree clumps from rangeland and for capturing diversity in rangeland structure and fire effects. Estimates of biomass burned derived from the airborne emissions sampling of carbon mass fluxes is currently ongoing (Bela et al., 2022; Kille et al., 2022), and in the future holds potential to derive independent estimates of the biomass burned from the smoke.

List of Abbreviations

ALS:	airborne laser scanning
BB-FLUX:	Biomass Burning Fluxes of Trace Gases and Aerosols
EVT:	Existing Vegetation Type
FACTS:	Forest Activity Tracking System
FCCS:	Fuel Characteristics Classification System
FFT:	Fuel and Fire Tools
GeoMAC:	Geospatial Multi-Agency Coordination
LF:	LANDFIRE
MBE:	mean bias error
NAWFD:	North American Wildland Fuel Database
NEON:	National Ecological Observatory Network
RF:	Random Forest
RMSE:	root mean squared error

Data Availability Statement

The fuel load and fuel consumption raster data using the ALS and FCCS approaches in this study are available at WIFIRE Commons via <https://doi.org/10.48792/W2RP4S> for the Keithly Fire data and <https://doi.org/10.48792/W2WC72> for the Tepee Fire data. These data were collected using funding from the U.S. Government and can be used without additional permissions or fees under Creative Commons Attribution 4.0. If you use these data in a publication, presentation, or other research product please use either the data citation or the journal article citation.

Acknowledgments

This research and the field data collection were funded by the Joint Fire Science Program (JFSP) Fire and Smoke Modeling of Emissions Experiment (FASMEE) Project (15-S-01-01). The post-fire ALS data collected/used in this research were obtained through the National Ecological Observatory Network (NEON) Assignable Assets program, a program sponsored by the National Science Foundation (NSF) and operated under cooperative agreement by Battelle. The BB-FLUX project and NEON data collection were supported by NSF awards AGS-1754019 and AGS-1842139.

References

- Alonzo, M., Morton, D. C., Cook, B. D., Andersen, H.-E., Babcock, C., & Pattison, R. (2017). Patterns of canopy and surface layer consumption in a boreal forest fire from repeat airborne lidar. *Environmental Research Letters*, 12(6), 065004. <https://doi.org/10.1088/1748-9326/aa6ade>
- Andersen, H.-E., McGaughey, R. J., & Reutebuch, S. E. (2005). Estimating forest canopy fuel parameters using LIDAR data. *Remote Sensing of Environment*, 94(4), 441–449. <https://doi.org/10.1016/j.rse.2004.10.013>
- Bela, M. M., Kille, N., McKeen, S. A., Romero-Alvarez, J., Ahmadov, R., James, E., et al. (2022). Quantifying Carbon Monoxide Emissions on the Scale of Large Wildfires. *Geophysical Research Letters*, 49(3), 1–11. <https://doi.org/10.1029/2021GL095831>
- Bonham, C. D. (1989). *Measurements for terrestrial vegetation*. John Wiley & Sons.
- Breiman, L. (2001). Random forests. *Machine Learning*, 45, 5–32. <https://doi.org/10.1023/a:1010933404324>
- Bright, B., Hudak, A., Meddens, A., Hawbaker, T., Briggs, J., & Kennedy, R. (2017). Prediction of forest canopy and surface fuels from lidar and satellite time series data in a bark beetle-affected forest. *Forests*, 8(9), 322. <https://doi.org/10.3390/f8090322>
- Brown, J. K., Oberhau, R. D., & Johnston, C. M. (1982). *Handbook for inventorying surface fuels and biomass in the Interior West*. In *General Technical Report INT-129*. USDA Forest Service, Intermountain Forest and Range Experiment Station.
- Campbell, J., Donato, D., Azuma, D., & Law, B. (2007). Pyrogenic carbon emission from a large wildfire in Oregon, United States. *Journal of Geophysical Research: Biogeosciences*, 112(4), 1–11. <https://doi.org/10.1029/2007JG000451>
- Cansler, C. A., Swanson, M. E., Furniss, T. J., Larson, A. J., & Lutz, J. A. (2019). Fuel dynamics after reintroduced fire in an old-growth Sierra Nevada mixed-conifer forest. *Fire Ecology*, 15(1), 16. <https://doi.org/10.1186/s42408-019-0035-y>
- Cardil, A., Monedero, S., Schag, G., De-Miguel, S., Tapia, M., Stoof, C. R., et al. (2021). Fire behavior modeling for operational decision-making. *Current Opinion in Environmental Science & Health*, 23(August), 100291. <https://doi.org/10.1016/j.coesh.2021.100291>

- Chuvieco, E., Mouillot, F., Van der Werf, G. R., San Miguel, J., Tanase, M., Koutsias, N., et al. (2019). Historical background and current developments for mapping burned area from satellite Earth observation. *Remote Sensing of Environment*, 225(November), 45–64. <https://doi.org/10.1016/j.rse.2019.02.013>
- Evens, J. S., & Murphy, M. A. (2017). *rfUtilities: Random forests model selection and performance evaluation*. Retrieved from <http://cran.r-project.org/package=rfUtilities>
- Fekety, P. A., Falkowski, M. J., & Hudak, A. T. (2015). Temporal transferability of LiDAR-based imputation of forest inventory attributes. *Canadian Journal of Forest Research*, 45(4), 422–435. <https://doi.org/10.1139/cjfr-2014-0405>
- Finney, M. A. (2001). Design of regular landscape fuel treatment patterns for modifying fire growth and behavior. *Forest Science*, 47(2), 219–228.
- Fire and Environmental Research Applications Team (2020). *Fuel and fire tools*. Retrieved from <https://www.fs.usda.gov/pnw/tools/fuel-and-fire-tools-fft>
- French, N. H. F., De Groot, W. J., Jenkins, L. K., Rogers, B. M., Alvarado, E., Amiro, B., et al. (2011). Model comparisons for estimating carbon emissions from North American wildland fire. *Journal of Geophysical Research: Biogeosciences*, 116(2). <https://doi.org/10.1029/2010JG001469>
- French, N. H. F., Goovaerts, P., & Kasichke, E. S. (2004). Uncertainty in estimating carbon emissions from boreal forest fires. *Journal of Geophysical Research*, 109. <https://doi.org/10.1029/2003JD003635>
- García, M., Riaño, D., Chuvieco, E., Salas, J., & Danson, F. M. (2011). Multispectral and LiDAR data fusion for fuel type mapping using support vector machine and decision rules. *Remote Sensing of Environment*, 115(6), 1369–1379. <https://doi.org/10.1016/j.rse.2011.01.017>
- García, M., Saatchi, S., Casas, A., Koltunov, A., Ustin, S., Ramirez, C., et al. (2017). Quantifying biomass consumption and carbon release from the California Rim fire by integrating airborne LiDAR and Landsat OLI data. *Journal of Geophysical Research: Biogeosciences*, 122(2), 340–353. <https://doi.org/10.1002/2015JG003315>
- García, M., Saatchi, S., Casas, A., Koltunov, A., Ustin, S., Ramirez, C., & Balzter, H. (2017). Extrapolating forest canopy fuel properties in the California rim fire by combining airborne LiDAR and Landsat OLI data. *Remote Sensing*, 9(4), 394. <https://doi.org/10.3390/rs9040394>
- Glenn, N. F., Neuenschwander, A., Vierling, L. A., Spaete, L., Li, A., Shinneman, D. J., et al. (2016). Landsat 8 and ICESat-2: Performance and potential synergies for quantifying dryland ecosystem vegetation cover and biomass. *Remote Sensing of Environment*, 185, 233–242. <https://doi.org/10.1016/j.rse.2016.02.039>
- Greaves, H. E., Vierling, L. A., Eitel, J. U. H., Boelman, N. T., Magney, T. S., Prager, C. M., & Griffin, K. L. (2016). High-resolution mapping of aboveground shrub biomass in Arctic tundra using airborne LiDAR and imagery. *Remote Sensing of Environment*, 184, 361–373. <https://doi.org/10.1016/j.rse.2016.07.026>
- Hiers, J. K., O'Brien, J. J., Mitchell, R. J., Grego, J. M., & Loudermilk, E. L. (2009). The wildland fuel cell concept: An approach to characterize fine-scale variation in fuels and fire in frequently burned longleaf pine forests. *International Journal of Wildland Fire*, 18(3), 315–325. <https://doi.org/10.1071/WF08084>
- Hoe, M. S., Dunn, C. J., & Temesgen, H. (2018). Multitemporal LiDAR improves estimates of fire severity in forested landscapes. *International Journal of Wildland Fire*, 27(9), 581. <https://doi.org/10.1071/WF17141>
- Hu, T., Ma, Q., Su, Y., Battles, J. J., Collins, B. M., Stephens, S. L., et al. (2019). A simple and integrated approach for fire severity assessment using bi-temporal airborne LiDAR data. *International Journal of Applied Earth Observation and Geoinformation*, 78(January), 25–38. <https://doi.org/10.1016/j.jag.2019.01.007>
- Hudak, A. T., Dickinson, M. B., Bright, B. C., Kremens, R. L., Loudermilk, E. L., O'Brien, J. J., et al. (2016). Measurements relating fire radiative energy density and surface fuel consumption—RxCADRE 2011 and 2012. *International Journal of Wildland Fire*, 25(1), 25–37. <https://doi.org/10.1071/WF14159>
- Hudak, A. T., Kato, A., Bright, B. C., Loudermilk, E. L., Hawley, C., Restaino, J. C., et al. (2020). Towards spatially explicit quantification of pre- and postfire fuels and fuel consumption from traditional and point cloud measurements. *Forest Science*, Xx, 1–15. <https://doi.org/10.1093/forsci/xfz085>
- Hudak, A. T., Strand, E. K., Vierling, L. A., Byrne, J. C., Eitel, J. U. H., Martinuzzi, S., & Falkowski, M. J. (2012). Quantifying aboveground forest carbon pools and fluxes from repeat LiDAR surveys. *Remote Sensing of Environment*, 123, 25–40. <https://doi.org/10.1016/j.rse.2012.02.023>
- Isenbourg, M. (2013). *LASTools – Efficient tools for LiDAR processing*. Retrieved from <http://lastools.org>
- Jakubowski, M. K., Guo, Q., Collins, B., Stephens, S., & Kelly, M. (2013). Predicting surface fuel models and fuel metrics using LiDAR. *Photogrammetric Engineering & Remote Sensing*, 79(1), 37–49. <https://doi.org/10.14358/pers.79.1.37>
- Jansen, V. S., Kolden, C. A., Greaves, H. E., & Eitel, J. U. H. (2019). Lidar provides novel insights into the effect of pixel size and grazing intensity on measures of spatial heterogeneity in a native bunchgrass ecosystem. *Remote Sensing of Environment*, 235(August), 111432. <https://doi.org/10.1016/j.rse.2019.111432>
- Keane, R. E., & Gray, K. (2013). Comparing three sampling techniques for estimating fine woody down dead biomass. *International Journal of Wildland Fire*, 22(8), 1093–1107. <https://doi.org/10.1071/WF13038>
- Keane, R. E., Herynk, J. M., Toney, C., Urbanski, S. P., Lutes, D. C., & Ottmar, R. D. (2013). Evaluating the performance and mapping of three fuel classification systems using forest inventory and analysis surface fuel measurements. *Forest Ecology and Management*, 305, 248–263. <https://doi.org/10.1016/j.foreco.2013.06.001>
- Kennedy, M. C., Prichard, S. J., McKenzie, D., & French, N. H. F. (2020). Quantifying how sources of uncertainty in combustible biomass propagate to prediction of wildland fire emissions. *International Journal of Wildland Fire*, 29(9), 793. <https://doi.org/10.1071/WF19160>
- Kille, N., Zarzana, K. J., Romero Alvarez, J., Lee, C. F., Rowe, J. P., Howard, B., et al. (2022). The CU Airborne Solar Occultation Flux Instrument: Performance Evaluation during BB-FLUX. *ACS Earth and Space Chemistry*, 6(3), 582–596. <https://doi.org/10.1021/acsearthspacechem.1c00281>
- Lentile, L. B., Holden, Z. A., Smith, A. M. S., Falkowski, M. J., Hudak, A. T., Morgan, P., et al. (2006). Remote sensing techniques to assess active fire characteristics and post-fire effects. *International Journal of Wildland Fire*, 15(3), 319–345. <https://doi.org/10.1071/WF05097>
- Li, A., Dhakal, S., Glenn, N. F., Spaete, L. P., Shinneman, D. J., Pilliod, D. S., et al. (2017). Lidar aboveground vegetation biomass estimates in shrublands: Prediction, uncertainties and application to coarser scales. *Remote Sensing*, 9(9), 903. <https://doi.org/10.3390/rs9090903>
- Li, F., Zhang, X., Kondragunta, S., & Roy, D. P. (2018). Investigation of the fire radiative energy biomass combustion coefficient: A comparison of polar and geostationary satellite retrievals over the conterminous United States. *Journal of Geophysical Research: Biogeosciences*, 123(2), 722–739. <https://doi.org/10.1002/2017JG004279>
- Lydersen, J. M., Collins, B. M., Knapp, E. E., Roller, G. B., & Stephens, S. (2015). Relating fuel loads to overstorey structure and composition in a fire-excluded Sierra Nevada mixed conifer forest. *International Journal of Wildland Fire*, 24(4), 484–494. <https://doi.org/10.1071/WF13066>
- Marssett, R. C., Qi, J., Heilman, P., Biedenbender, S. H., Carolyn Watson, M., Amer, S., et al. (2006). Remote sensing for grassland management in the arid southwest. *Rangeland Ecology & Management*, 59(5), 530–540. <https://doi.org/10.2111/05-201R.1>

- McCarley, T. R., Hudak, A. T., Sparks, A. M., Vaillant, N. M., Meddens, A. J. H., Trader, L., et al. (2020). Estimating wildfire fuel consumption with multitemporal airborne laser scanning data and demonstrating linkage with MODIS-derived fire radiative energy. *Remote Sensing of Environment*, *251*, 112114. <https://doi.org/10.1016/j.rse.2020.112114>
- McCarley, T. R., Smith, A. M. S. S., Kolden, C. A., & Kreidler, J. (2018). Evaluating the mid-infrared bi-spectral Index for improved assessment of low-severity fire effects in a conifer forest. *International Journal of Wildland Fire*, *27*(6), 407–412. <https://doi.org/10.1071/WF17137>
- McKenzie, D., Raymond, C. L., Kellogg, L.-K. B., Norheim, R. A., Andreu, A. G., Bayard, A. C., et al. (2007). Mapping fuels at multiple scales: Landscape application of the fuel characteristic classification system. *Canadian Journal of Forest Research*, *37*(12), 2421–2437. <https://doi.org/10.1139/X07-056>
- Mundt, J. T., Streutker, D. R., & Glenn, N. F. (2006). Mapping sagebrush distribution using fusion of hyperspectral and LiDAR classifications. *Photogrammetric Engineering & Remote Sensing*, *72*(1), 47–54. <https://doi.org/10.14358/PERS.72.1.47>
- Murphy, M. A., Evans, J. S., & Storf, A. (2010). Quantifying Bufo boreas connectivity in Yellowstone National Park with landscape genetics. *Ecology*, *91*(1), 252–261. <https://doi.org/10.1890/08-0879.1>
- Ottmar, R. D. (2014). Wildland fire emissions, carbon, and climate: Modeling fuel consumption. *Forest Ecology and Management*, *317*, 41–50. <https://doi.org/10.1016/j.foreco.2013.06.010>
- Ottmar, R. D., Burns, M. F., Hall, J. N., & Hanson, A. D. (1993). CONSUME users guide. *Tech. Rep. PNW-GTR-304*. U.S. Department of Agriculture, Forest Service.
- Ottmar, R. D., Sandberg, D. V., Riccardi, C. L., & Prichard, S. J. (2007). An overview of the fuel characteristic classification system — quantifying, classifying, and creating fuelbeds for resource planning. *Canadian Journal of Forest Research*, *37*(12), 2383–2393. <https://doi.org/10.1139/X07-077>
- Pesonen, A., Maltamo, M., Eerikäinen, K., & Packalèn, P. (2008). Airborne laser scanning-based prediction of coarse woody debris volumes in a conservation area. *Forest Ecology and Management*, *255*(8–9), 3288–3296. <https://doi.org/10.1016/j.foreco.2008.02.017>
- Pettinari, M. L., & Chuvieco, E. (2016). Generation of a global fuel data set using the Fuel Characteristic Classification System. *Biogeosciences*, *13*(7), 2061–2076. <https://doi.org/10.5194/bg-13-2061-2016>
- Price, O. F., & Gordon, C. E. (2016). The potential for LiDAR technology to map fire fuel hazard over large areas of Australian forest. *Journal of Environmental Management*, *181*, 663–673. <https://doi.org/10.1016/j.jenvman.2016.08.042>
- Prichard, S. J., Kennedy, M. C., Andreu, A. G., Eagle, P. C., French, N. H., & Billmire, M. (2019). Next-generation biomass mapping for regional emissions and carbon inventories: Incorporating uncertainty in wildland fuel characterization. *Journal of Geophysical Research: Biogeosciences*, *124*(12), 3699–3716. <https://doi.org/10.1029/2019JG005083>
- Prichard, S. J., Larkin, N., Ottmar, R., French, N., Baker, K., Brown, T., et al. (2019). The fire and smoke model evaluation experiment—A plan for integrated, large fire-atmosphere field campaigns. *Atmosphere*, *10*(2), 66. <https://doi.org/10.3390/atmos10020066>
- Prichard, S. J., Sandberg, D. V., Ottmar, R. D., Eberhardt, E., Andreu, A., Eagle, P., & Swedin, K. (2013). *Classification System Version 3.0: Technical Documentation*. U.S. Department of Agriculture, Forest Service.
- Reinhardt, E., Scott, J., Gray, K., & Keane, R. (2006). Estimating canopy fuel characteristics in five conifer stands in the Western United States using tree and stand measurements. *Canadian Journal of Forest Research*, *36*(11), 2803–2814. <https://doi.org/10.1139/x06-157>
- Reinhardt, E. D., & Crookston, N. L. (2003). *Fire and fuels extension to the forest vegetation simulator*. USDA Forest Service. General Technical Report RMRS-GTR-116.
- Riaño, D., Chuvieco, E., Condés, S., González-Matesanz, J., & Ustin, S. L. (2004). Generation of crown bulk density for *Pinus sylvestris* L. from lidar. *Remote Sensing of Environment*, *92*(3), 345–352. <https://doi.org/10.1016/j.rse.2003.12.014>
- Riaño, D., Chuvieco, E., Salas, J., Palacios-Orueta, A., & Bastarrica, A. (2002). Generation of fuel type maps from Landsat TM images and ancillary data in Mediterranean ecosystems. *Canadian Journal of Forest Research*, *32*(8), 1301–1315. <https://doi.org/10.1139/x02-052>
- Riaño, D., Meier, E., & Allgower, B. (2003). Modeling airborne laser scanning data for the spatial generation of critical forest parameters in fire behavior modeling. *Remote Sensing of Environment*, *86*(2), 177–186. [https://doi.org/10.1016/S0034-4257\(03\)00098-1](https://doi.org/10.1016/S0034-4257(03)00098-1)
- Riccardi, C. L., Ottmar, R. D., Sandberg, D. V., Andreu, A., Elman, E., Kopper, K., & Long, J. (2007). The fuelbed: A key element of the fuel characteristic classification system. *Canadian Journal of Forest Research*, *37*(12), 2394–2412. <https://doi.org/10.1139/X07-143>
- Rollins, M. G. (2009). LANDFIRE: A nationally consistent vegetation, wildland fire, and fuel assessment. *International Journal of Wildland Fire*, *18*(3), 235. <https://doi.org/10.1071/WF08088>
- Roussel, J.-R., & Auty, D. (2019). *lidR: Airborne LiDAR data manipulation and visualization for forestry applications*. Retrieved from <https://cran.r-project.org/package=lidR>
- Simard, M., Pinto, N., Fisher, J. B., & Baccini, A. (2011). Mapping forest canopy height globally with spaceborne lidar. *Journal of Geophysical Research: Biogeosciences*, *116*(4), 1–12. <https://doi.org/10.1029/2011JG001708>
- Skowronski, N. S., Clark, K. L., Duveneck, M., & Hom, J. (2011). Three-dimensional canopy fuel loading predicted using upward and downward sensing LiDAR systems. *Remote Sensing of Environment*, *115*(2), 703–714. <https://doi.org/10.1016/j.rse.2010.10.012>
- Skowronski, N. S., Gallagher, M. R., & Warner, T. A. (2020). Decomposing the interactions between fire severity and canopy fuel structure using multi-temporal, active, and passive remote sensing approaches. *Fire*, *3*(7), 21. <https://doi.org/10.3390/fire3010007>
- Spaete, L. P., Glenn, N. F., Derryberry, D. R., Sankey, T. T., Mitchell, J. J., & Hardegree, S. P. (2011). Vegetation and slope effects on accuracy of a LiDAR-derived DEM in the sagebrush steppe. *Remote Sensing Letters*, *2*(4), 317–326. <https://doi.org/10.1080/01431161.2010.515267>
- Sparks, A. M., Boschetti, L., Smith, A. M. S., Tinkham, W. T., Lannom, K. O., & Newingham, B. A. (2015). An accuracy assessment of the MTBS burned area product for shrub-steppe fires in the northern Great Basin, United States. *International Journal of Wildland Fire*, *24*(1), 70. <https://doi.org/10.1071/WF14131>
- Trigg, S., & Flasse, S. (2001). An evaluation of different bi-spectral spaces for discriminating burned shrub-savannah. *International Journal of Remote Sensing*, *22*(13), 2641–2647. <https://doi.org/10.1080/01431160110053185>
- USDA Forest Service. (2020). Forest activity tracking system. Retrieved from <https://data.fs.usda.gov/geodata/edw/datasets>
- Van Der Werf, G. R., Randerson, J. T., Giglio, L., Van Leeuwen, T. T., Chen, Y., Rogers, B. M., et al. (2017). Global fire emissions estimates during 1997–2016. *Earth System Science Data*, *9*(2), 697–720. <https://doi.org/10.5194/essd-9-697-2017>
- Volkamer, R., Kille, N., Lee, C. F., Zarzana, K. J., Koenig, T., Nutter, R., et al. (2020). The BB-FLUX Project: How much fuel goes up in smoke? *American Meteorological Society 100th Annual Meeting*.
- Wang, C., & Glenn, N. F. (2009). Estimation of fire severity using pre- and post-fire LiDAR data in sagebrush steppe rangelands. *International Journal of Wildland Fire*, *18*(7), 848–856. <https://doi.org/10.1071/WF08173>
- Woodall, C. W., & Monleon, V. J. (2010). Estimating the quadratic mean diameters of fine woody debris in forests of the United States. *Forest Ecology and Management*, *260*(6), 1088–1093. <https://doi.org/10.1016/j.foreco.2010.06.036>

- Zhang, K., Chen, S. C., Whitman, D., Shyu, M. L., Yan, J., & Zhang, C. (2003). A progressive morphological filter for removing nonground measurements from airborne LIDAR data. *IEEE Transactions on Geoscience and Remote Sensing*, *41*(4I), 872–882. <https://doi.org/10.1109/TGRS.2003.810682>
- Zhao, K., Suarez, J. C., Garcia, M., Hu, T., Wang, C., & Londo, A. (2018). Utility of multitemporal lidar for forest and carbon monitoring: Tree growth, biomass dynamics, and carbon flux. *Remote Sensing of Environment*, *204*(September), 883–897. <https://doi.org/10.1016/j.rse.2017.09.007>